International Journal for Uncertainty Quantification, 5 (3): 255–273 (2015)

STOCHASTIC GALERKIN METHODS AND MODEL ORDER REDUCTION FOR LINEAR DYNAMICAL SYSTEMS

***Roland Pulch*[1,*] *& E. Jan W. ter Maten*[2,3]**

[1] *Department of Mathematics and Computer Science, Ernst-Moritz-Arndt-Universität Greifswald, Walther-Rathenau-Straße 47, D-17487 Greifswald, Germany*

[2] *Centre for Analysis, Scientific computing and Applications (CASA), Dept. Mathematics & Computer Science, Technische Universiteit Eindhoven, P.O.Box 513, NL-5600 MB Eindhoven, The Netherlands*

[3] *Chair of Applied Mathematics and Numerical Analysis (FB C, AMNA), Bergische Universität Wuppertal, Gaußstraße 20, D-42119 Wuppertal, Germany*

Original Manuscript Submitted: 10/15/2013; Final Draft Received: 03/02/2015

Linear dynamical systems are considered in the form of ordinary differential equations or differential algebraic equations. We change their physical parameters into random variables to represent uncertainties. A stochastic Galerkin method yields a larger linear dynamical system satisfied by an approximation of the random processes. If the original systems own a high dimensionality, then a model order reduction is required to decrease the complexity. We investigate two approaches: the system of the stochastic Galerkin scheme is reduced and, vice versa, the original systems are reduced followed by an application of the stochastic Galerkin method. The properties are analyzed in case of reductions based on moment matching with the Arnoldi algorithm. We present numerical computations for two test examples.

KEY WORDS: *stochastic modeling, polynomial chaos, stochastic Galerkin method, model order reduction, quadrature, dynamical systems, uncertainty quantification*

1. INTRODUCTION

In science and engineering, dynamical systems of ordinary differential equations (ODEs) or differential algebraic equations (DAEs) often appear as mathematical models. The systems include physical parameters, which may exhibit uncertainties due to measurement errors or imperfections of a manufacturing procedure, for example. We quantify the uncertainties using a stochastic modeling, where the deterministic parameters are substituted by random variables.

The solution of the stochastic models can be computed numerically by sampling methods like (quasi) Monte Carlo simulations, for example. Therein, the dynamical system has to be solved many times. Alternatively, we consider numerical techniques based on the polynomial chaos expansion of the unknown random processes, see [1–3]. A stochastic Galerkin (SG) method yields a larger coupled system, which has to be solved just once to obtain an approximation of the random processes, see [4, 5]. This approach has already been applied successfully to systems of ODEs and DAEs, see [6–8].

We consider linear dynamical systems with random parameters, where the dimension of the state space is already large due to the original modeling. Thus a model order reduction (MOR) is advantageous to decrease the complexity of the problem. Appropriate MOR methods are available for linear dynamical systems, see [9–11]. Moreover, parameterized model order reduction (pMOR) has been developed to preserve deterministic parameters as independent

*Correspond to Roland Pulch, E-mail: pulchr@uni-greifswald.de, URL: http://www.math-inf.uni-greifswald.de

2152–5080/15/$35.00

variables in the reduced order models, see [12–15]. In case of large numbers of random parameters, a reduction of the random space based on a sensitivity analysis is discussed in [16]. Furthermore, reduced basis methods have been investigated for partial differential equations with stochastic influences in [17, 18], for example.

In this paper, we apply MOR in connection to the SG method to solve the stochastic models. The reduction of the coupled system resulting from the SG approach is investigated. This strategy has already been used in [19, 20] for Gaussian random variables. We reduce the original dynamical systems and apply the SG method afterward. In the second approach, more variants are feasible. We discuss both traditional MOR and pMOR for this purpose. A focus is on reduction using moment matching by the Arnoldi algorithm, see [21], which turns out to be advantageous due to a preservation of smoothness. A brief error analysis is given. We compare the two strategies with respect to accuracy and computational effort.

2. DYNAMICAL SYSTEMS WITH RANDOM PARAMETERS

In this section, we define the problems to be considered in the stochastic methods and the model order reduction.

2.1 Linear Dynamical Systems

We consider linear dynamical systems of the form

$$\begin{aligned} C(p)\dot{x}(t,p) + G(p)x(t,p) &= Bu(t) \\ y(t,p) &= Lx(t,p) \end{aligned} \tag{1}$$

in a time interval $t \in [t_0, t_1]$ with input signals $u : [t_0, t_1] \to \mathbb{R}^{N_{\mathrm{in}}}$ from some class. The square matrices $C(p), G(p) \in \mathbb{R}^{N \times N}$ typically include physical parameters $p \in \Pi$ in some relevant subset $\Pi \subseteq \mathbb{R}^Q$. Consequently, the unknown state variables $x : [t_0, t_1] \times \Pi \to \mathbb{R}^N$ depend on time as well as the parameters. Furthermore, output variables $y : [t_0, t_1] \times \Pi \to \mathbb{R}^{N_{\mathrm{out}}}$ are defined as quantities of interest. The matrices $B \in \mathbb{R}^{N \times N_{\mathrm{in}}}$ and $L \in \mathbb{R}^{N_{\mathrm{out}} \times N}$ are associated to the input and the output, respectively, and often do not depend on physical parameters. Thus we assume that B and L are constant. Nevertheless, generalizations to parameter-dependent matrices are straightforward.

In mathematical models of technical applications, and assuming appropriate definitions of the parameters, the entries of the matrices $C(p), G(p)$ in (1) are often polynomials or even affine-linear functions in the variables p. For example, modified nodal analysis [22] for linear electric circuits yields systems (1), where the matrices are affine-linear functions of capacitances, inductances and conductances. In [7, 23], parameter-dependent matrices like $C(p)$ are assumed to be of the form

$$C(p) = C_0 + \eta_1(p_1)C_1 + \cdots + \eta_Q(p_Q)C_Q, \tag{2}$$

(and similarly for $G(p)$) with linear or nonlinear scalar functions η_j and examples are given.

We assume either $\det(C(p)) \neq 0$ for all $p \in \Pi$ or $\det(C(p)) = 0$ for all $p \in \Pi$. Thus the system (1) represents either ordinary differential equations (ODEs) or differential algebraic equations (DAEs) only. In the latter case, we suppose a regular matrix pencil, i.e., it holds for each $p \in \Pi$ that $\det(G(p) + \lambda C(p)) \neq 0$ for all $\lambda \in \mathbb{C} \backslash T(p)$ with some finite set $T(p) \subset \mathbb{C}$. We omit the mixed case of regular and singular matrices $C(p)$ for simplicity, since it hardly appears in practice. Nevertheless, most of the following results also apply to the mixed case.

Let $U(s)$, $X(s,p)$, $Y(s,p)$ be the Laplace transforms of the above time-dependent functions with the same dimensions. The input-output behavior of the dynamical system (1) is specified by a transfer function in the frequency domain, see [9]. Due to the dependence on the parameters, the transfer function reads as

$$H(s,p) = L(G(p) + sC(p))^{-1}B \tag{3}$$

with the variable $s \in \mathbb{C} \backslash T(p)$. The transfer function is matrix-valued, since it holds that $H(s,p) \in \mathbb{C}^{N_{\mathrm{out}} \times N_{\mathrm{in}}}$. An exception are single-input-single-output (SISO) systems, which imply $N_{\mathrm{out}} = N_{\mathrm{in}} = 1$. The input-output relation is given by $Y(s,p) = H(s,p)U(s)$ in any case.

2.2 Stochastic Modeling

Now we assume that the chosen parameters exhibit some uncertainties. Following a common approach in uncertainty quantification, we substitute the parameters by independent random variables

$$p : \Omega \to \Pi, \quad \omega \mapsto p(\omega) = (p_1(\omega), \dots, p_Q(\omega))^\top$$

on some probability space $(\Omega, \mathcal{A}, P)$ with event space Ω, sigma-algebra $\mathcal{A}$, and probability measure P. We assume continuous random variables in the following, for example, uniformly distributed, Gaussian-distributed or beta-distributed functions. Generalizations to discrete random variables are feasible, cf. [5, Ch. 3.1]. Using continuous random variables, a probability density function $\rho : \Pi \to \mathbb{R}$ is available. Consequently, the state variables and outputs satisfying (1) become time-dependent random processes. We are interested in statistics (expected value, variance, etc.) or more sophisticated stochastic quantities of the outputs.

Given a measurable function $f : \Pi \to \mathbb{K}$ with $\mathbb{K} = \mathbb{R}$ or $\mathbb{K} = \mathbb{C}$, we introduce the abbreviation

$$\mathrm{E}\left[f(p)\right] := \int_\Omega f(p(\omega)) \, \mathrm{d}P(\omega) = \int_\Pi f(p)\rho(p) \, \mathrm{d}p \tag{4}$$

for the expected value, provided that it exists. The expected value (4) implies an inner product for the Hilbert space $L^2(\Pi, \rho) := \{f : \Pi \to \mathbb{K} \,|\, \mathrm{E}[|f|^2] < \infty\}$. Given $f, g \in L^2(\Pi, \rho)$, this inner product is just

$$\langle f(p), g(p) \rangle := \mathrm{E}\Big[f(p)g(p)\Big] \quad \text{for } \mathbb{K} = \mathbb{R} \quad \text{and} \quad \langle f(p), g(p) \rangle := \mathrm{E}\Big[f(p)\overline{g(p)}\Big] \quad \text{for } \mathbb{K} = \mathbb{C}.$$

We apply this notation also to vector-valued as well as matrix-valued functions $f(p) \in \mathbb{K}^{M \times N}$ and scalar functions $g(p) \in \mathbb{K}$, where $\langle f(p), g(p) \rangle \in \mathbb{K}^{M \times N}$ is defined componentwise by $\langle f_{ij}(p), g(p) \rangle$. Furthermore, the inner product defines a norm $\| \cdot \|_{L^2}$ on $L^2(\Pi, \rho)$.

2.3 Polynomial Chaos Expansion

Each probability distribution yields an associated orthonormal system of polynomials $(\Phi_i)_{i \in \mathbb{N}}$ provided that all polynomials belong to $L^2(\Pi, \rho)$, see [1]. Thus it holds that $\langle \Phi_i(p), \Phi_j(p) \rangle = \delta_{ij}$ with the Kronecker delta δ_{ij}. Furthermore, let $\Phi_0 \equiv 1$ be the constant polynomial. We assume that the orthonormal polynomials are dense in $L^2(\Pi, \rho)$. This property is fulfilled by probability distributions of uniform, Gaussian or beta type, for example. General distributions have to satisfy certain conditions, see [24], whereas a treatment of lognormal distributions can be found in [25]. Consequently, a function $f \in L^2(\Pi, \rho)$ exhibits a representation in the so-called polynomial chaos (PC), see [5],

$$f(p) = \sum_{i=0}^{\infty} f_i \Phi_i(p), \tag{5}$$

in which the coefficients $f_i \in \mathbb{K}$ are given by the projection $f_i = \langle f(p), \Phi_i(p) \rangle$. The expansion (5) converges in the norm of $L^2(\Pi, \rho)$. The rate of convergence depends on the smoothness of f with respect to the parameters. The expected value is just $\mathrm{E}[f] = f_0$. For $\mathbb{K} = \mathbb{R}$, the variance follows from an infinite sum: $\mathrm{Var}(f) = f_1^2 + f_2^2 + \cdots$.

Assuming functions in $L^2(\Pi, \rho)$, we apply the PC expansion (5) to the state variables, the output variables, and the transfer function of the dynamical system (1). Therein, the representation exists pointwise for each time $t \in [t_0, t_1]$ or each frequency $s \in \mathbb{C}$.

To compute an approximation of the random processes x or y solving (1), a PC expansion (5) is truncated after the first M terms. Typically, all basis polynomials $\Phi_0, \dots, \Phi_{M-1}$ up to some degree D are chosen. It holds that $M = (Q + D)!/Q!D!$.

The rate of convergence of the expansion (5) depends on the smoothness of the function f with respect to the parameters p, see [5, Thm. 3.6], for example. Given a k-times weakly differentiable function on a compact domain Π, the truncation error is proportional to D^{-k}.

There are mainly two types of numerical methods to compute the unknown coefficient functions: stochastic collocation techniques and the stochastic Galerkin (SG) method, see [2, 4, 5]. We consider only the SG approach in this paper, since its properties are advantageous in the case of linear dynamical systems, see [26]. However, we admit that in several cases the stochastic collocation method combines providing good results with flexibility in allowing the use of different simulation tools.

2.4 Stochastic Galerkin Method

We outline the well-known SG technique for the dynamical system (1) including random parameters. The PC expansion of the state variables as well as the output variables are truncated at some $M \geq 1$, i.e., we obtain

$$x^{(M)}(t,p) = \sum_{i=0}^{M-1} v_i(t)\Phi_i(p), \quad y^{(M)}(t,p) = \sum_{i=0}^{M-1} w_i(t)\Phi_i(p). \tag{6}$$

It holds that $w_i(t) = Lv_i(t)$ for the original coefficients only, i.e., the equality is violated if the exact coefficients are replaced by approximations. Inserting the finite sums (6) into the linear dynamical system (1) yields the residuals

$$\begin{aligned} \delta_x(t,p) &:= C(p)\dot{x}^{(M)}(t,p) + G(p)x^{(M)}(t,p) - Bu(t), \\ \delta_y(t,p) &:= y^{(M)}(t,p) - Lx^{(M)}(t,p). \end{aligned}$$

We want to determine the unknown coefficients such that the residuals become small in some sense. The Galerkin method implies that the residuals are orthogonal with respect to the applied space of basis polynomials, i.e.,

$$\langle \delta_x(t,p), \Phi_l(p) \rangle = 0, \quad \langle \delta_y(t,p), \Phi_l(p) \rangle = 0 \qquad \text{for } l = 0, 1, \ldots, M-1$$

and each $t \in [t_0, t_1]$.

Since every involved function is assumed to be continuous in time, it is reasonable to consider all $t \in [t_0, t_1]$. We obtain the larger coupled system

$$\begin{aligned} \hat{C}\dot{v}(t) + \hat{G}v(t) &= \hat{B}u(t) \\ w(t) &= \hat{L}v(t) \end{aligned} \tag{7}$$

with $v := (v_0, v_1, \ldots, v_{M-1})^\top \in \mathbb{R}^{MN}$ and $w := (w_0, w_1, \ldots, w_{M-1})^\top \in \mathbb{R}^{MN_{\mathrm{out}}}$. The resulting matrices $\hat{C}, \hat{G} \in \mathbb{R}^{MN \times MN}$ consist of the following minors

$$\begin{aligned} \hat{C} &= (\hat{C}_{ij})_{i,j=0,\ldots,M-1}, \quad \hat{C}_{ij} := \langle C(p)\Phi_i(p), \Phi_j(p) \rangle, \\ \hat{G} &= (\hat{G}_{ij})_{i,j=0,\ldots,M-1}, \quad \hat{G}_{ij} := \langle G(p)\Phi_i(p), \Phi_j(p) \rangle. \end{aligned} \tag{8}$$

The matrices $\hat{B} \in \mathbb{R}^{MN \times N_{\mathrm{in}}}$ and $\hat{L} \in \mathbb{R}^{MN_{\mathrm{out}} \times MN}$ are $\hat{B} = (1, 0, \ldots, 0)^\top \otimes B$ and $\hat{L} = I_M \otimes L$ with the Kronecker product and the identity matrix I_M, since their entries do not depend on the parameters. The coupled system (7) has to be solved just once to achieve an approximation of the random processes.

Assuming a decomposition (2), in which the required scalar functions are polynomials, we can calculate the entries (8) of the matrices $\hat{C}, \hat{G}$ in (7) analytically for traditional probability distributions. In any case, we can use a quadrature for the probabilistic integrals in (8) to compute the entries of $\hat{C}, \hat{G}$ sufficiently accurate a priori, while the computational effort is often negligible in comparison to the time integration or a reduction of the coupled system (7).

The coupled system (7) also exhibits an input-output behavior, which is specified by the transfer function

$$\hat{H}(s) := \hat{L}(\hat{G} + s\hat{C})^{-1}\hat{B}. \tag{9}$$

It follows that the entries of $\hat{H}(s) \in \mathbb{C}^{MN_{\mathrm{out}} \times N_{\mathrm{in}}}$ include approximations of the PC coefficients for the original transfer function (3), see [16].

2.5 Model Order Reduction

We now assume that the dynamical system (1) has a huge dimensionality N. The following statements also hold for deterministic parameters. Let first a fixed realization $p \in \Pi$ of the parameters be given. Several approaches exist to reduce the complexity of such systems like moment matching, Krylov-space methods, balanced truncation, SVD-type methods, proper orthogonal decomposition, see [9]. It follows that the system (1) is reduced to a system

$$\begin{aligned} C_r(p)\dot{x}_r(t,p) + G_r(p)x_r(t,p) &= B_r(p)u(t) \\ y_r(t,p) &= L_r(p)x_r(t,p) \end{aligned} \tag{10}$$

of state space dimension $N_{\mathrm{red}} \ll N$.

Yet good approximations $y_r \approx y$ are desired, which is conditional to the proper choice of the matrices in the reduced system. The transfer function of the reduced order model (10) reads as

$$H_r(s,p) := L_r(G_r(p) + sC_r(p))^{-1}B_r \tag{11}$$

with same size $\mathbb{C}^{N_{\mathrm{out}} \times N_{\mathrm{in}}}$ as H in (3). Often the MOR approach yields projection matrices $W(p), V(p) \in \mathbb{C}^{N \times N_{\mathrm{red}}}$ satisfying the orthogonality condition $W^{\mathrm{H}}(p)V(p) = I_{N_{\mathrm{red}}}$ such that

$$\begin{aligned} C_r(p) &= W(p)^{\mathrm{H}}C(p)V(p), & G_r(p) &= W(p)^{\mathrm{H}}G(p)V(p), \\ B_r(p) &= W(p)^{\mathrm{H}}B, & L_r(p) &= LV(p). \end{aligned} \tag{12}$$

Note that the matrices B_r and L_r depend on the parameters now due to the projection matrices.

We consider moment matching for MOR, based on Krylov-spaces. The accuracy of these techniques focuses on the imaginary axis in the frequency domain, see [27–29]. For simplicity, we will restrict ourselves in choosing a suitable expansion point $s_0 = \mathrm{i}\omega_0$ with $\omega_0 \in \mathbb{R}$ (a point for which the matrix pencil is nonsingular). We note that interpolation (expansion) points for rational interpolation methods (moment matching methods) are often chosen off the imaginary axis. For example, a real expansion point implies that all computations are real. With complex expansion points one can tune the accuracy. When optimal interpolation points are sought, they are usually somewhere in the complex plane, cf. [27, 28]. Of course, in the end, one must take care that a real problem is approximated by a real reduced model. A detailed discussion can be found in [27, Section 7].

Optimal expansion points reduce the number of moments that have to be matched. By this, the reduced models may be more sparse than by those derived with fixed expansion points. However, optimal expansion points are often parameter-dependent. We assume expansion points that are fixed for all parameters under study. This property can be easily generalized to the case that the set of expansion points over all parameters is finite.

Choosing an expansion point $s_0 = \mathrm{i}\omega_0$ with $\omega_0 \in \mathbb{R}$, the reduced order model (10) is constructed such that the transfer function H_r becomes a Padé approximant of H with identical moments in s_0 up to some order. We will use the Arnoldi process to calculate the projection matrices, which implies $W(p) = V(p)$. Generalizations to several expansion points also exist. For more details, we refer to [9, 21, 27]. This strategy is also applicable to the coupled system (7) in the same manner.

Alternatively, techniques of parameterized model order reduction (pMOR) preserve the parameters as independent variables in reduced systems, see [12, 14, 15, 30]. Often constant projection matrices $W_0, V_0 \in \mathbb{C}^{N \times N_{\mathrm{red}}}$ are determined a priori using the information from many samples of the parameters, cf. [35], for example. The matrices of the reduced order model (10) become

$$\begin{aligned} C_r(p) &= W_0^{\mathrm{H}}C(p)V_0, & G_r(p) &= W_0^{\mathrm{H}}G(p)V_0, \\ B_r &= W_0^{\mathrm{H}}B, & L_r &= LV_0. \end{aligned} \tag{13}$$

An advantage is that an explicit formula is available for $C_r(p), G_r(p)$ and arbitrary $p \in \Pi$. The evaluation of this formula becomes cheap if the number of parameter-dependent entries is much smaller than the number of constant entries in the matrices $C(p), G(p)$, which allows for projecting the parameter-independent part a priori in the offline phase of the MOR. Furthermore, the matrices B_r, L_r are independent of the parameters.

3. REDUCTION OF THE STOCHASTIC MODEL

In this section, we investigate two approaches that are illustrated in Table 1. In Section 3.1, we first apply the SG method to the random dynamical system and next use MOR methods (first "right," then "down"). In Section 3.2, we first employ a (parameterized) MOR method and next apply the SG method (first "down," then "right").

3.1 MOR for the SG System

The SG method changes the random dynamical system (1) into the coupled system (7). If the size N of the original system is already large, then the coupled system exhibits the even higher dimension MN. Hence the coupled system (7) is an excellent candidate for MOR. Moreover, a high potential for reduction appears, because sparse representations are often observed in a PC expansion, see [31, 32]. If the number M refers to all polynomials up to a fixed degree, then a sparse representation implies that a smaller number of basis functions would also yield an approximation of the same quality. Ordinary MOR schemes for the coupled system (7) are able to decrease the dimensionality without knowing the significant basis polynomials. In particular, a potential for MOR is given even if the original system (1) does not allow for an efficient reduction. Note that there is no need for pMOR schemes in this procedure, since the parameters do not appear explicitly in the coupled system (7) due to the probabilistic integration in (8).

MOR of the coupled system (7) yields a linear dynamical system of smaller size

$$\begin{aligned} \hat{C}_r \dot{v}_r(t) + \hat{G}_r v_r(t) &= \hat{B}_r u(t) \\ w_r(t) &= \hat{L}_r v_r(t). \end{aligned} \tag{14}$$

This strategy was already applied in [19, 20] for random variables with Gaussian distributions. In [16], this reduction has been employed for uniformly distributed parameters.

We consider moment matching for a reduction of the system (7), where the Arnoldi algorithm is applied, see [21]. We suppose that all resulting linear systems of algebraic equations are solved directly by an LU-decomposition. Assuming a single expansion point $s_0 \in \mathbb{C}$, this procedure requires just one decomposition of the matrix $\hat{G} + s_0\hat{C}$, cf. (9). However, if the dimension MN is huge, then this decomposition represents a bottleneck in the complete strategy.

3.1.1 Convergence Properties

To analyze the performance of this approach, we investigate the relations between the transfer functions of the systems (1) and (7). For simplicity, we consider SISO systems, since generalizations to multiple-input-multiple-output are straightforward. A result on the Laplace transform is required.

TABLE 1: Flow chart

$C(p)\dot{x} + G(p)x = Bu$ $y = Lx$	SG $\longrightarrow$	$\hat{C}\dot{v} + \hat{G}v = \hat{B}u$ $w = \hat{L}v$
$Y(s,p) = H(s,p)U(s)$		$W(s) = \hat{H}(s)U(s)$
(p)MOR $\downarrow$		MOR $\downarrow$
$C_r(p)\dot{x}_r + G_r(p)x_r = B_r(p)u$ $y_r = L_r(p)x_r$	SG $\longrightarrow$	$\hat{C}_r\dot{v}_r + \hat{G}_r v_r = \hat{B}_r u$ $w_r = \hat{L}_r v_r$
$Y_r(s,p) = H_r(s,p)U(s)$		$W_r(s) = \hat{H}_r(s)U(s)$

Lemma 1 (Laplace transform)**.** *Let $y(t,p)$ and a sequence $y^{(M)}(t,p)$ for the integers $M \geq 1$ be given, where all functions are in $L^2(\Pi,\rho)$ for each $t \geq 0$. In addition, the Laplace transforms of the time variable for all those functions and each $p \in \Pi$ are assumed to exist for all $s \in \mathbb{C}$ satisfying $\mathrm{Re}(s) > \alpha$ with a constant $\alpha \in \mathbb{R}$ independent of M and p. If the convergence*

$$\lim_{M\to\infty} \left\| y^{(M)}(t,\cdot) - y(t,\cdot) \right\|_{L^2} = 0 \qquad \textit{for each } \ t \geq 0 \tag{15}$$

is valid and dominated by a function $z \in L^1([0,\infty))$, i.e.,

$$0 \leq \left\| y^{(M)}(t,\cdot) - y(t,\cdot) \right\|_{L^2} \leq z(t) \qquad \textit{for all } \ t \geq 0 \ \textit{ and all } \ M \geq 1,$$

then the associated Laplace transforms inherit the convergence

$$\lim_{M\to\infty} \left\| Y^{(M)}(s,\cdot) - Y(s,\cdot) \right\|_{L^2} = 0 \qquad \textit{for each } \ s \in \mathbb{C} \ \textit{ with } \ \mathrm{Re}(s) > \max\{\alpha, 0\}. \tag{16}$$

Proof. We write

$$\begin{aligned}
&\left\| Y^{(M)}(s,\cdot) - Y(s,\cdot) \right\|_{L^2}^2 \\
&= \int_\Pi \left| \int_0^\infty \mathrm{e}^{-st} y^{(M)}(t,p)\, \mathrm{d}t - \int_0^\infty \mathrm{e}^{-st} y(t,p)\, \mathrm{d}t \right|^2 \rho(p)\, \mathrm{d}p \\
&\leq \int_\Pi \left[\int_0^\infty \left| \mathrm{e}^{-st} (y^{(M)}(t,p) - y(t,p)) \right| \, \mathrm{d}t \right]^2 \rho(p)\, \mathrm{d}p \\
&= \int_\Pi \left[\int_0^\infty \int_0^\infty \left| \mathrm{e}^{-sv} \mathrm{e}^{-su} (y^{(M)}(v,p) - y(v,p))(y^{(M)}(u,p) - y(u,p)) \right| \, \mathrm{d}u\mathrm{d}v \right] \rho(p)\, \mathrm{d}p
\end{aligned} \tag{17}$$

for each $s \in \mathbb{C}$ with $\mathrm{Re}(s) > \alpha$, while the existence of this upper estimate is not guaranteed yet. The Cauchy-Schwarz inequality yields

$$\begin{aligned}
&\int_0^\infty \int_0^\infty \left[\int_\Pi \left| \mathrm{e}^{-sv} \mathrm{e}^{-su} (y^{(M)}(v,p) - y(v,p))(y^{(M)}(u,p) - y(u,p)) \right| \, \rho(p)\, \mathrm{d}p \right] \, \mathrm{d}u\mathrm{d}v \qquad (18) \\
&= \int_0^\infty \int_0^\infty \left| \mathrm{e}^{-sv} \mathrm{e}^{-su} \right| \cdot \left\langle \left| y^{(M)}(v,p) - y(v,p) \right|, \left| y^{(M)}(u,p) - y(u,p) \right| \right\rangle \, \mathrm{d}u\mathrm{d}v \\
&\leq \int_0^\infty \int_0^\infty \left| \mathrm{e}^{-sv} \right| \cdot \left| \mathrm{e}^{-su} \right| \cdot \left\| y^{(M)}(v,\cdot) - y(v,\cdot) \right\|_{L^2} \cdot \left\| y^{(M)}(u,\cdot) - y(u,\cdot) \right\|_{L^2} \, \mathrm{d}u\mathrm{d}v \\
&\leq \left[\int_0^\infty \left\| y^{(M)}(t,\cdot) - y(t,\cdot) \right\|_{L^2} \, \mathrm{d}t \right]^2,
\end{aligned}$$

for each $s \in \mathbb{C}$ with $\mathrm{Re}(s) > \max\{\alpha, 0\}$. The final integral in time exists due to the assumption of the dominating function z. The existence of the upper bound also shows that the integrals (18) exist. Hence the integral (18) is equal to the integral (17) for each M by the theorem of Fubini. It follows that

$$\left\| Y^{(M)}(s,\cdot) - Y(s,\cdot) \right\|_{L^2} \leq \int_0^\infty \left\| y^{(M)}(t,\cdot) - y(t,\cdot) \right\|_{L^2} \, \mathrm{d}t, \qquad \text{for all } \ M \geq 1$$

and each $s \in \mathbb{C}$ with $\mathrm{Re}(s) > \max\{\alpha, 0\}$. For increasing M, the integrand of the upper bound converges point-wise to zero for each $t \geq 0$ due to (15). We obtain the convergence (16) by the theorem of dominated convergence. □

We continue by showing that the transfer function of the coupled system converges to the original transfer function of the random dynamical system provided that the SG method converges in time domain.

Theorem 1 (Convergence of transfer function)**.** *Let the stochastic Galerkin method be convergent in the time domain, i.e., the sequence $y^{(M)}(t,p)$ of outputs satisfies (15). Under the additional assumptions of Lemma 1, it follows that*

$$\lim_{M\to\infty} \left\| H(s,\cdot) - \sum_{i=0}^{M-1} \hat{H}_i(s)\Phi_i(\cdot) \right\|_{L^2} = 0 \qquad \textit{for each } \; s\in\mathbb{C} \; \textit{ with } \; \mathrm{Re}(s) > \max\{\alpha,0\}, \tag{19}$$

where $H(s,p)$ is the transfer function of the dynamical system (1) and $\hat{H}_i(s)$ are the values from (9) belonging to the coupled system (7).

Proof. Let $w_i(t)$ for $i = 0,1,\ldots,M-1$ be the components of the output of the coupled system (7), which means that they are not identical to the exact PC coefficients. Let $W_i(s)$ be the Laplace transform of $w_i(t)$ for each i. The approximation $y^{(M)}(t,p)$ is reconstructed from $w_0(t),\ldots,w_{M-1}(t)$. Its Laplace transform can be written as

$$Y^{(M)}(s,p) = \sum_{i=0}^{M-1} W_i(s)\Phi_i(p)$$

due to the linearity of the Laplace transformation. The convergence (15) implies the convergence (16) of the associated Laplace transforms by Lemma 1. Given an arbitrary input u and its Laplace transform U, we obtain

$$\begin{aligned} \left\| Y(s,\cdot) - Y^{(M)}(s,\cdot) \right\|_{L^2}^2 &= \left\| H(s,\cdot)U(s) - \sum_{i=0}^{M-1} \hat{H}_i(s)U(s)\Phi_i(\cdot) \right\|_{L^2}^2 \\ &= |U(s)|^2 \cdot \left\| H(s,\cdot) - \sum_{i=0}^{M-1} \hat{H}_i(s)\Phi_i(\cdot) \right\|_{L^2}^2 \end{aligned}$$

for each $s\in\mathbb{C}$ where the Laplace transform exists. For each fixed s_0, we choose the input $u(t) := \mathrm{e}^{(-1+s_0)t}$, which results in $U(s_0) = 1$. Hence the convergence (19) follows pointwise for s. □

3.1.2 Error analysis

We analyze the approximation error for the transfer function. Let $\|\cdot\|_{L^2}$ be the norm of the Hilbert space $L^2(\Pi,\rho)$ for complex-valued functions. We denote the components of the transfer function for the reduced system (14) by $(\hat{H}_r)_i$. It follows that

$$\begin{aligned} &\left\| H(s,\cdot) - \sum_{i=0}^{M-1} (\hat{H}_r)_i(s)\Phi_i(\cdot) \right\|_{L^2} \\ &\le \left\| H(s,\cdot) - \sum_{i=0}^{M-1} \hat{H}_i(s)\Phi_i(\cdot) \right\|_{L^2} + \left\| \sum_{i=0}^{M-1} \left[\hat{H}_i(s) - (\hat{H}_r)_i(s) \right] \Phi_i(\cdot) \right\|_{L^2} =: \; E_1(s) + E_2(s). \end{aligned} \tag{20}$$

The term E_1 in (20) converges to zero in view of Theorem 1. The term E_2 in (20) can be estimated by

$$E_2(s) \le \sum_{i=0}^{M-1} \left| \hat{H}_i(s) - (\hat{H}_r)_i(s) \right| = \left\| \hat{H}(s) - \hat{H}_r(s) \right\|_1$$

with the vector norm $\|\cdot\|_1$ in $\mathbb{C}^M$, since each basis polynomial has an L^2-norm of one. The magnitude of the error term E_2 depends on the MOR scheme applied to the coupled system (7).

3.2 MOR for Original Parameterized System

Now we reduce the dynamical system (1) at first and use the SG method afterward. The strategy from Section 3.1 is straightforward except for the choice of the MOR scheme. In contrast, the alternative strategy of this subsection allows for several variants with respect to the discretization of probabilistic integrals in the SG technique. Moreover, the feasibility of each approach has to be examined carefully.

We assume that a method of MOR yields the matrices in the reduced system (10) of dimension N_{red} for an arbitrary $p \in \Pi$. A direct application of the SG method to the system (10) results in the following formulas for the minors of the matrices:

$$\begin{aligned}
\hat{C}_r \in \mathbb{C}^{MN_{\mathrm{red}} \times MN_{\mathrm{red}}} &: (\hat{C}_r)_{ij} := \langle C_r(p)\Phi_i(p), \Phi_j(p)\rangle, \\
\hat{G}_r \in \mathbb{C}^{MN_{\mathrm{red}} \times MN_{\mathrm{red}}} &: (\hat{G}_r)_{ij} := \langle G_r(p)\Phi_i(p), \Phi_j(p)\rangle, \\
\hat{B}_r \in \mathbb{C}^{MN_{\mathrm{red}} \times N_{\mathrm{in}}} &: (\hat{B}_r)_{i} := \langle B_r(p), \Phi_i(p)\rangle, \\
\hat{L}_r \in \mathbb{C}^{MN_{\mathrm{out}} \times MN_{\mathrm{red}}} &: (\hat{L}_r)_{ij} := \langle L_r(p)\Phi_i(p), \Phi_j(p)\rangle.
\end{aligned} \tag{21}$$

The matrices are real-valued or complex-valued conditioned by the MOR scheme.

In (21), we assume the existence of the probabilistic integrals. If the matrices of the reduced order model are continuous in p and the space Π is compact, then this existence is guaranteed. We discuss two variants in the further proceeding.

3.2.1 Matrix Sampling

The probabilistic integrals in (21) are approximated by a quadrature formula or a sampling scheme. The approximation with respect to $\hat{C}_r$ reads as

$$\langle C_r(p)\Phi_i(p), \Phi_j(p)\rangle \doteq \sum_{k=1}^{K} \gamma_k C_r(p^{(k)})\Phi_i(p^{(k)})\Phi_j(p^{(k)})$$

with nodes $p^{(1)}, \ldots, p^{(K)} \in \Pi$ and weights $\gamma_1, \ldots, \gamma_K \in \mathbb{R}$. Likewise, the identical quadrature is used for the other matrices. Hence the computational work consists of K reductions of the system (1). It is natural to apply the same MOR approach pointwise for each node $p^{(k)}$ to determine the reduced matrices. Using moment matching, the dimension of the Krylov-spaces may depend on p. However, an identical reduced dimension N_{red} is assumed for all nodes in our approach.

For the existence of the probabilistic integrals in (21), we assume that the reduced matrices are at least continuous with respect to the dependence on the parameters, cf. [12]. Note that there may be some MOR approaches, where this property is violated. Nevertheless, the smoothness of the matrices with respect to parameters is preserved by the Arnoldi procedure.

Lemma 2 (Matrices from Arnoldi algorithm)**.** *In the moment matching technique, let the same expansion point $s_0 \in \mathbb{C}$ be chosen such that $G(p) + s_0 C(p)$ is regular for all $p \in \Pi$. Assume that the dimensions of the Krylov-spaces are at least N_{red} for all $p \in \Pi$. If the matrices $C(p), G(p)$ are ℓ-times continuously differentiable on the parameter space Π, then the Arnoldi algorithm yields a projection matrix $V(p) \in \mathbb{R}^{N \times N_{\mathrm{red}}}$ that is ℓ-times continuously differentiable again.*

Proof. Without loss of generality, we assume a single input ($B \in \mathbb{R}^N \backslash \{0\}$). Using $F(p) := G(p) + s_0 C(p)$, it holds that $F, F^{-1} \in \mathcal{C}^\ell$ due to $C, G \in \mathcal{C}^\ell$. The moment matching can be done employing the Krylov-subspaces $\mathcal{K}_m(A(p), b(p))$ with $A(p) := F(p)^{-1}C(p)$ and $b(p) := -F(p)^{-1}B$, see [21, Section 3]. Let $m = N_{\mathrm{red}}$. It holds that $b(p) \neq 0$ due to $B \neq 0$. In addition, we obtain $A, b \in \mathcal{C}^\ell$.

We apply the Arnoldi algorithm from [9, p. 335]. The initialization reads as

$$v_1 := \frac{b(p)}{\|b(p)\|}, \quad w(p) := A(p)v_1(p), \quad \alpha(p) := v_1(p)^{\mathrm{H}} w(p), \quad r_1(p) := w(p) - \alpha(p)v_1(p), \quad V_1(p) := (v_1(p)).$$

Obviously, all operations are differentiable and thus preserve the smoothness. For $j = 1, \ldots, m-1$, the algorithm proceeds by

$$v_{j+1}(p) := \frac{r_j(p)}{\|r_j(p)\|}, \quad V_{j+1}(p) := (V_j(p)\ v_{j+1}(p)), \quad w(p) := A(p)v_{j+1}(p),$$
$$h(p) := V_{j+1}(p)^H w(p), \quad r_{j+1}(p) := w(p) - V_{j+1}(p)h(p).$$

Again all operations yield smooth functions. The assumption on the dimension of the Krylov-subspaces guarantees the property $r_j(p) \neq 0$ for $j = 1, \ldots, m-1$. It follows that $V \in \mathcal{C}^\ell$. □

Note that the compactness of the parameter space Π is sufficient for the existence of expansion points (also on the imaginary axis) satisfying our assumption in case of a regular matrix pencil for all p. In practical computations, the Arnoldi algorithm should be terminated if tiny vectors $r_j(p)$ occur in view of numerical stability. Therefore, one has to assume that these vectors are sufficiently large up to order N_{red} for all $p \in \Pi$.

Now Lemma 2 implies that the reduced matrices $C_r(p), G_r(p), B_r(p), L_r(p)$ in (12) inherit the smoothness. The information from Lemma 2 is valuable, since it allows for conclusions on the convergence of the SG method in case of ODEs (1). If $C(p), G(p) \in \mathcal{C}^\ell$, then the solution satisfies $x, y \in \mathcal{C}^\ell$ with respect to the parameters. The speed of convergence of the PC expansion depends on the smoothness of the random processes. Now the Arnoldi algorithm implies a reduced system (10). We assume that $C_r(p)$ is regular, which is obvious in case of symmetric positive definite matrices $C(p)$, for example. Hence the solution fulfills $x_r, y_r \in \mathcal{C}^\ell$ again. Although the SG method is convergent for just continuous reduced matrices, the rate of convergence of the SG is preserved due to the smoothness. In case of DAEs (1), the analysis of the dependence on parameters is more difficult and the index of the system has to be considered, cf. [33].

3.2.2 Parameterized MOR approach

Now we employ a pMOR as outlined in Section 2.5. Given constant projection matrices $W_0, V_0 \in \mathbb{C}^{N \times N_{\mathrm{red}}}$, we arrange the reduced matrices (13). The computation of the reduced matrices (21) in the SG method can be done exactly now. We obtain

$$\langle C_r(p)\Phi_i(p), \Phi_j(p)\rangle \ = \ \langle W_0 C(p) V_0 \Phi_i(p), \Phi_j(p)\rangle \ = \ W_0 \langle C(p)\Phi_i(p), \Phi_j(p)\rangle V_0 \ = \ W_0 \hat{C}_{ij} V_0$$

and, likewise, for the other matrices. Since the projection matrices are constant, the existence of the probabilistic integrals follows directly from the continuity of the matrices $C(p), G(p)$.

We recognize the minors (8) of the matrix of the coupled system (7) in the above formula. Thus the reduced matrices can be written as

$$\begin{aligned} \hat{C}_r &= (I_M \otimes W_0)^{\mathrm{H}} \hat{C} (I_M \otimes V_0), & \hat{G}_r &= (I_M \otimes W_0)^{\mathrm{H}} \hat{G} (I_M \otimes V_0), \\ \hat{B}_r &= (I_M \otimes W_0)^{\mathrm{H}} \hat{B}, & \hat{L}_r &= \hat{L} (I_M \otimes V_0) \end{aligned} \tag{22}$$

using Kronecker products and the identity matrix I_M. Hence the construction (22) represents a special case of MOR for the coupled system (7), cf. Section 3.1. The crucial advantage is that an LU-decomposition of a matrix of size MN is omitted in this variant.

We consider two techniques to construct the projection matrices, which will be used for numerical simulations in Section 4. Therein, we arrange $W_0 = V_0$.

a) A trivial pMOR is obtained by using $V_0 := V(\overline{p})$ with some reference realization $\overline{p} \in \Pi$ of the parameters like the expected value $\overline{p} := \mathrm{E}[p]$, for example. The computational effort consists of just a single application of a scheme for MOR. However, we do not expect a high accuracy in this variant unless the projection matrix $V(p)$ is nearly constant with respect to the parameters. We refer to [13, 34] for a good example of a projection matrix $V(p)$ that strongly varies with respect to p.

b) A more sophisticated approach uses samples $p^{(1)}, \dots, p^{(K)} \in \Pi$, where the reduction is applied pointwise. A grid of a quadrature rule can also be used to obtain this discrete set of parameters, although the quadrature weights usually do not appear in the technique. It is allowed that the reduced dimension is different for each grid point now. For brevity, we assume the same dimension in each system. We arrange the projection matrices in a larger matrix

$$\tilde{V} := \left(V(p^{(1)}) \cdots V(p^{(K)}) \right) \in \mathbb{C}^{N \times K N_{\mathrm{red}}}, \tag{23}$$

in which each individual $V(p^{(j)})$ is a nonsquare matrix with orthonormal columns. In [35], the pMOR was performed by the global matrix $V_0 := \tilde{V}$ obtained by explicit moment matching after expanding in all components of p. A stable implicit moment matching algorithm is provided in [13]. A recycling Krylov-space approach is considered in [15]. Using all these algorithms, one may stop a particular extension of the subspace built so far when the new vector orthogonal to it has a sufficiently small norm.

Also we consider an additional reduction, since the dimension KN_{red} of (23) may be large. We follow an approach used in [12, 36], where a global basis was constructed from several local bases. A singular value decomposition (SVD) yields the factorization $\tilde{V} = UDT^{\mathrm{H}}$ with unitary matrices U, T and a diagonal matrix D including the singular values. The span of the column vectors satisfies $\mathrm{span}(\tilde{V}) = \mathrm{span}(UD)$. Choosing an integer $R < KN_{\mathrm{red}}$, we collect the R columns of U, which correspond to the largest singular values, into a global projection matrix $V_0 \in \mathbb{C}^{N \times R}$. Thus we obtain the dominant directions in V_0.

By enlarging the spaces, in separating real parts and imaginary parts of basis vectors, real projection matrices can be derived if desired, cf. [13].

3.2.3 Error Analysis

We discuss shortly the error of the techniques from Section 3.2.1 and Section 3.2.2. Similar to (20), it follows that

$$\begin{aligned} &\left\| H(s,\cdot) - \sum_{i=0}^{M-1} (\hat{H}_r)_i(s) \Phi_i(\cdot) \right\|_{L^2} \\ &\leq \left\| H(s,\cdot) - H_r(s,\cdot) \right\|_{L^2} + \left\| H_r(s,\cdot) - \sum_{i=0}^{M-1} (\hat{H}_r)_i(s) \Phi_i(\cdot) \right\|_{L^2} =: \; E_3(s) + E_4(s). \end{aligned} \tag{24}$$

The quality of the MOR determines the magnitude of the term $E_3(s)$ in (24). Since the L^2-norm of the probability space is employed, the MOR is required to be sufficiently accurate in subdomains of the parameters with relatively large probabilities. The term $E_4(s)$ in (24) depends on the convergence of the SG method. Using the Arnoldi procedure, the SG approach is convergent for systems of ODEs (1), due to Lemma 2. Theorem 1 implies that $E_4(s)$ tends to zero.

3.3 Comparison

Finally, Table 2 summarizes the properties of the two approaches. The first strategy indicates a higher accuracy, while a large computational effort appears for large numbers of basis polynomials. Vice versa, the second strategy offers a lower computational time, whereas the accuracy is reduced by further errors.

In both approaches, the PC expansions (5) are truncated after M terms. The examinations of this section imply results on the convergence properties for $M \to \infty$. In practice, the degree of the truncation should be chosen such that the output of the system (1) is approximated sufficiently accurate. In many applications, increasing the variance of the input random parameters requires to select a higher polynomial degree, i.e., a larger M is needed.

4. TEST EXAMPLES

We present results for the simulation of two illustrative examples in this section.

TABLE 2: Comparison of the two approaches in Section 3.1 and Section 3.2

MOR after SG	SG after MOR
often high potential for reduction of the coupled system	potential for reduction depends only on the parameterized system
matrices $\hat{G}, \hat{C}$ often computable without errors	matrices $\hat{G}_r, \hat{C}_r$ include some discretization error
arbitrary choice of reduced dimension	system has to be reduced to the same dimension for each parameter in matrix sampling
LU-decomposition of higher dimension MN	LU-decompositions of dimension N
potential for parallelism mostly just in LU-decomposition	potential for parallelism by MOR for different parameters

4.1 Anemometer

The anemometer represents a benchmark in the MOR Wiki [37]. A fluid is heated up, where a flow field causes an asymmetric heat distribution. Consequently, a temperature difference appears between two thermal sensors, which allows for a measurement of the fluid velocity. Figure 1 illustrates the layout of the anemometer.

This application is modeled by a convection-diffusion equation

$$\rho c \frac{\partial T}{\partial t} = \nabla \cdot (\kappa \nabla T) - \rho c \, \vec{v} \cdot \nabla T + \dot{q} \tag{25}$$

for the unknown temperature T in two space dimensions. The heat flow $\dot{q}$ represents the input, whereas the temperature difference of the sensors yields the output. A velocity profile $\vec{v}$ is predetermined. The involved physical parameters are the density ρ, the scalar fluid velocity v (as a part of $\vec{v}$), the specific heat c, and the thermal conductivity κ. We assume a constant density $\rho = 1$. Hence our parameters read as $p = (v, c, \kappa)^\top$. A finite element discretization of the partial differential equation (25) produces an implicit system of ODEs with dimension $N = 29{,}008$. This SISO system exhibits the following dependence on the parameters

$$\begin{aligned} C(c)\dot{x}(t,p) + G(v,c,\kappa)x(t,p) &= Bu(t), \\ y(t,p) &= Lx(t,p). \end{aligned}$$

The regular matrix C is diagonal, whereas the matrix G is sparse but asymmetric. The entries of C are affine functions of c and the entries of G represent polynomials up to degree two in the parameters. L selects the temperature difference between the two sensors. These matrices are directly obtained from [37]. More details on this example can be found in [38].

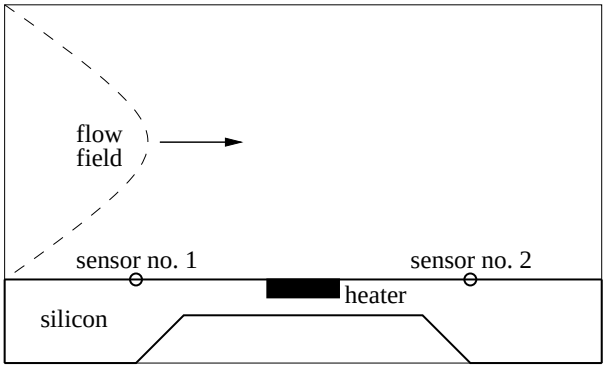

FIG. 1: Layout of the anemometer.

We replace the parameters $p = (v, c, \kappa)^\top$ by independent uniformly distributed random variables with 5% variation around the mean values $\overline{v} = 1$, $\overline{c} = 1/2$, $\overline{\kappa} = 3/2$. In the PC expansion, we use all multivariate Legendre polynomials up to degree two, i.e., $M = 10$ basis functions appear. Thus the coupled system (7) owns the dimension $MN = 290{,}080$.

In each reduced order model, we consider moment matching at the expansion point $s_0 = \mathrm{i}\omega_0$ with $\omega_0 = 1$ and apply the Arnoldi algorithm. The coupled system (7) is reduced to dimension 500. Each original system (1) is decreased to size $N_{\mathrm{red}} = 100$. In the matrix sampling from Section 3.2.1, we apply a three-dimensional Gauss-Legendre quadrature with 27 nodes. In the pMOR approach from Section 3.2.2, the expected value for p is chosen to provide a reference realization. For the SVD variant, we apply the grid of the Gaussian quadrature again and choose the dimension $R = 150$.

In each approach, we obtain approximations for the coefficients of the PC expansion of the transfer function. For a rough comparison of the accuracy in each method, the expected value and the standard deviation of the transfer function are reconstructed by the coefficients separately for real part and imaginary part. As a reference solution, these statistics of the transfer function are evaluated without reduction using a three-dimensional Gauss-Legendre quadrature with 125 nodes.

The transfer function is nearly constant outside some sufficiently large frequency interval, because it represents a rational function with a degree of the denominator larger or equal than the degree of the numerator. As error estimate, the maximum

$$\max_{\omega\in[\omega_1,\omega_2]} \left| \mathrm{E}\Big[\mathrm{Re}(\tilde{H}(\mathrm{i}\omega, p))\Big] - \mathrm{E}\Big[\mathrm{Re}(H(\mathrm{i}\omega, p))\Big] \right| \tag{26}$$

is employed with $\tilde{H}$ being the approximation of H. Likewise, the real part is replaced by the imaginary part and the expected value in (26) is changed into the standard deviation.

We consider the frequency interval $\omega \in [10^{-2}, 10^6]$. The maxima (26) are approximated on a fine grid within this frequency window. Table 3 shows the maximum differences of the approximations to the reference solution. Figure 2 depicts the expected value just for the reference solution, since the other methods produce almost the same result. For the standard deviation, larger differences appear, which are illustrated by Fig. 3. Indeed, for $\omega > 10^6$, we recognize a

TABLE 3: Maximum differences of approximations to reference solution in the frequency interval $\omega \in [10^{-2}, 10^6]$ for the anemometer

	Real/ex.v.	Imag./ex.v.	Real/st.d.	Imag./st.d.
MOR after SG	2.5e-02	2.5e-02	2.45e-01	2.62e-01
Matrix sampling	2.0e-02	2.1e-02	1.6e-02	1.7e-02
pMOR (a)	3.1e-02	2.4e-02	9.25e-01	7.44e-01
pMOR (b)	5.6e-02	3.7e-02	7.10e-01	4.36e-01

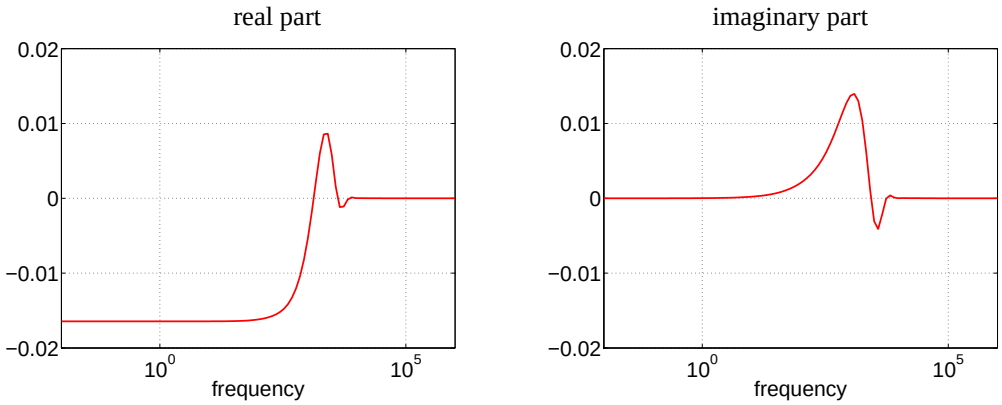

FIG. 2: Expected value of the transfer function for the anemometer.

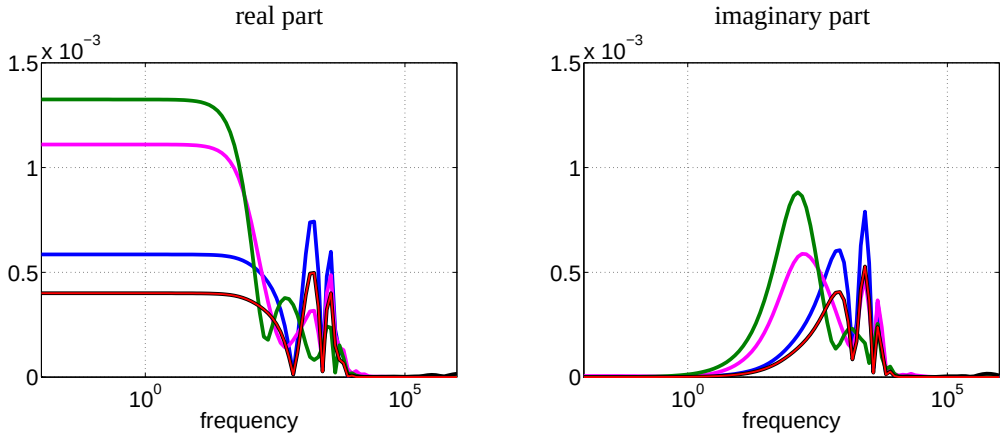

FIG. 3: Standard deviation of the transfer function for the anemometer: reference solution (red), MOR after SG (blue), matrix sampling (black), pMOR-a (green), and pMOR-b (magenta).

constant mean and a negligible variance. Also, the results by the matrix sampling approach nearly coincide with the reference solution, except for small differences, which appear far from the expansion point. Thus the matrix sampling is superior in this test example.

We present some more results on the pMOR method of Section 3.2.2 involving the SVD. Figure 4 shows the computed singular values of the matrix (23) as a decreasing sequence. We observe a rapid decay of the singular values after the first $N_{\mathrm{red}} = 100$ numbers, which indicates a high potential for reduction. The first $R = 150$ singular values make up 99.7% of the sum of all singular values.

We have done all calculations within the software package MATLAB on a computer including an Intel Core i5-4670 CPU, 3.40 GHz and operating system Kubuntu 14.04. The CPU times required for the above methods are depicted in Table 4. The work for the calculation of the matrices (8) in the SG approach, which is used in all MOR methods except for the matrix sampling, is shown separately. We present also relative computing times, where the method pMOR (a) is defined as reference, since it is the fastest technique in this example. The MOR of the SG system is the most expensive approach, since the work is dominated by the LU-decomposition of a huge matrix.

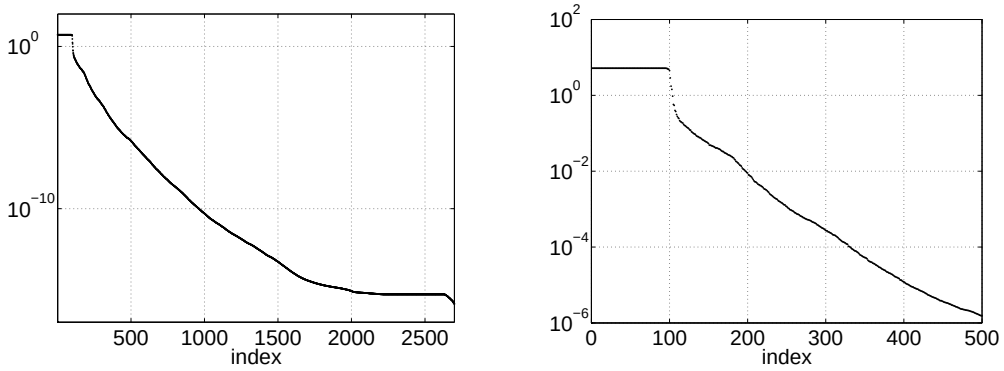

FIG. 4: Singular values of the matrix (23) appearing in pMOR for the anemometer: all values (left) and zoom (right).

TABLE 4: Computing times in methods applied to the anemometer example

	MOR after SG	Matrix sampling	pMOR (a)	pMOR (b)	SG matrices
CPU times	1359	308	84	734	5
Relative times	16.2	3.7	1.0	8.7	0.06

4.2 RLC Circuit

We apply a linear electric network from [39] shown in Fig. 5. This circuit consists of a repetition of N_{cell} cells and contains N_{cell} capacitances, $N_{\text{cell}} - 1$ inductances, N_{cell} conductances as well as two additional conductances at the boundaries. A voltage source yields the input signal and the current through this source represents the output signal. The modified nodal analysis, see [40], generates an SISO system (1) consisting of DAEs with index one. Therein, the matrices $C(p), G(p)$ are affine functions with respect to the physical parameters. The dimension of the state space becomes $N = 2N_{\text{cell}} + 1$.

We choose $N_{\text{cell}} = 10$ and substitute all physical parameters by random variables except for the two boundary conductances. Thus $Q = 29$ random parameters are involved, where we arrange independent uniform distributions with variations of 10% around the mean values 10^{-9} for capacitances, 10^{-6} for inductances, and unity for conductances. In the PC expansion, all multivariate Legendre polynomials up to degree two are used, resulting in $M = 465$ basis functions. Hence the SG method produces a coupled system (7) with $MN = 9{,}765$ equations. The involved matrices $\hat{C}, \hat{G}$ can be calculated analytically.

In each MOR approach, the expansion point $s_0 = \mathrm{i}\omega_0$ with $\omega_0 = 10^6$ is used. The method from Section 3.1 reduces the system (7) to a system of just 40 equations. For the techniques from Section 3.2, the potential for MOR of the system (1) is low now, since a relatively small dimension of the state space occurs. We select $N_{\text{red}} = 10$, which implies reduced systems of size $MN_{\text{red}} = 4650$ at the end. The Stroud quadrature of order 3, see [41], yields the matrix sampling. For some alternative quadrature approaches, see [25]. In the formula of Stroud, $K = 58$ nodes are located in the parameter space. For the first pMOR method, the expected value gives us the reference parameter again. For the second pMOR method, we reapply the grid from the Stroud quadrature. While all systems (1) are reduced to the dimension $N_{\text{red}} = 10$, the 12 dominating directions are selected from the SVD. For comparison, we calculate reference solutions without reduction using the Stroud quadrature of order 5, see [41], where $1{,}683$ nodes occur in the 29-dimensional parameter space.

We compare the statistics of the transfer functions for each reduction in the large frequency interval $\omega \in [1, 10^{15}]$. Figures 6 and 7 illustrate the expected values and the standard deviations, respectively. We recognize a good agreement of all methods around the expansion point and for smaller frequencies. The matrix sampling technique produces bad approximations for the variance at higher frequencies. We also analyze the differences for the separate complex-valued PC coefficients of the transfer function in the smaller frequency interval $\omega \in [10^5, 10^7]$ around the expansion point. The absolute values of the maximum differences are shown in Table 5, where the maximum is taken both in the frequency domain and in each group of the coefficients with respect to the degree of the associated basis polynomials. Now the matrix sampling features the best approximations. However, the reduced system of the matrix sampling is much larger than the reduced system from the technique of Section 3.1. The agreement of the differences for the pMOR approaches and the MOR after SG reflects that the pMOR can be seen as a special case of this technique due to (22).

We also present the singular values of the second pMOR approach in Fig. 8. Since the dimension of the state space is low, the number of singular values is equal to N now due to $N < KN_{\text{red}}$. The values do not decline rapidly after the first $N_{\text{red}} = 10$ entries, which indicates a low potential for reduction in this method. Nevertheless, the choice

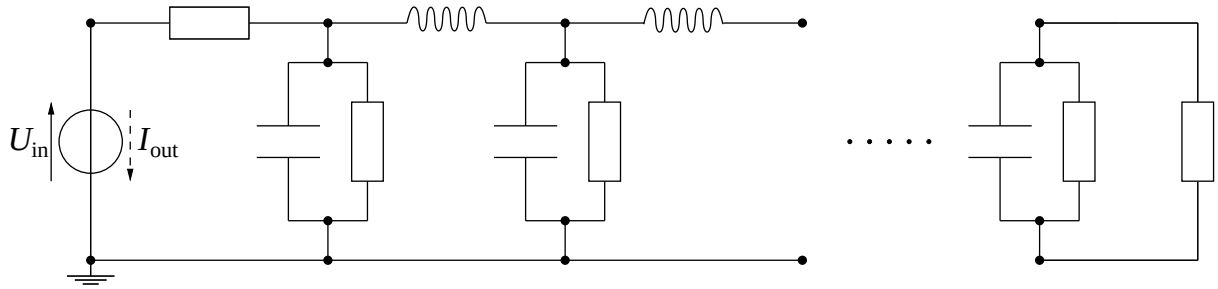

FIG. 5: Diagram of RLC circuit.

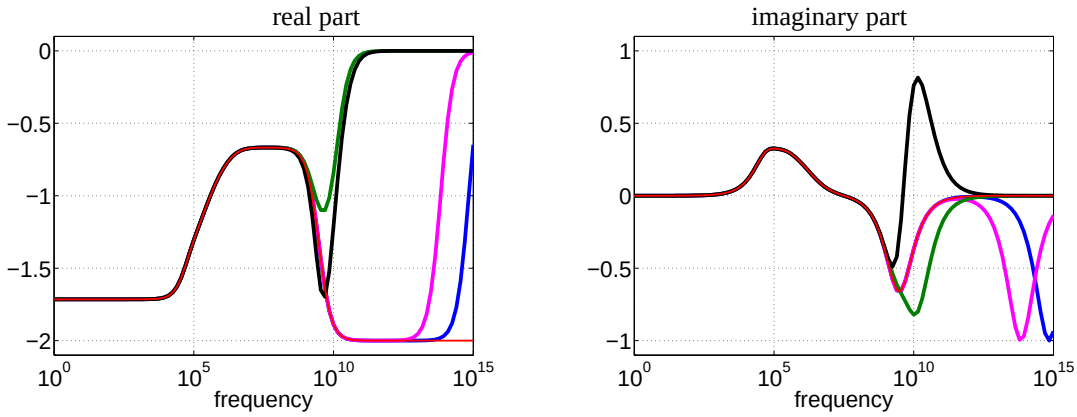

FIG. 6: Expected value of the transfer function for the RLC circuit: reference solution (red), MOR after SG (blue), matrix sampling (black), pMOR-a (green), and pMOR-b (magenta).

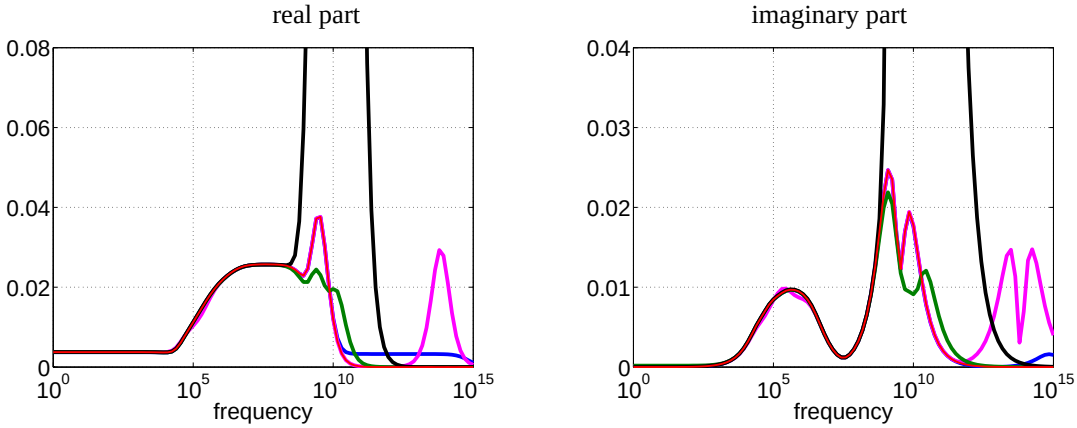

FIG. 7: Standard deviation of the transfer function for the RLC circuit: reference solution (red), MOR after SG (blue), matrix sampling (black), pMOR-a (green), and pMOR-b (magenta).

TABLE 5: Maximum differences of approximations to reference solution for the PC coefficients of the transfer function in the frequency interval $\omega \in [10^5, 10^7]$ for the RLC circuit

	Degree zero	Degree one	Degree two
MOR after SG	1.4606e-03	5.3744e-05	1.3181e-03
Matrix sampling	1.8314e-06	3.1944e-05	8.8125e-04
pMOR (a)	1.4735e-03	5.1020e-02	1.3180e-03
pMOR (b)	1.4887e-03	5.1031e-02	1.3181e-03

of $R = 12$ dominant directions yields much better approximations than the first pMOR variant with just a reference parameter for frequencies up to $\omega \approx 10^{11}$.

Finally, we present the observed computing times in Table 6 following the structure of Table 4. The reduction of the original systems (1) is cheap in this example. Since many basis polynomials appear, the effort for the calculation of the SG matrices is dominating due to summations within the minors (8). Now the matrix sampling exhibits the highest computational work, because the formation of the matrices is a part of the method, whereas the time for the SG matrices as input is separated from the other approaches.

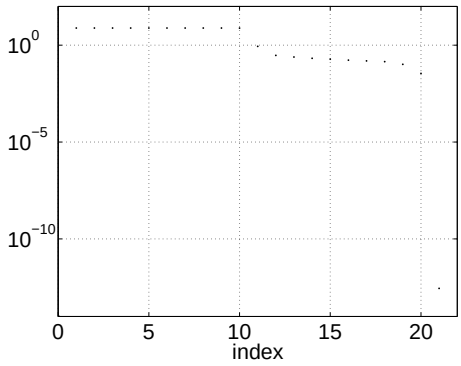

FIG. 8: Singular values of the matrix (23) appearing in pMOR of RLC circuit.

TABLE 6: Computing times in methods applied to the circuit example

	MOR after SG	Matrix sampling	pMOR (a)	pMOR (b)	SG matrices
CPU times	6.1	22.2	0.03	0.1	26.7
Relative times	203	740	1.0	3.3	890

5. CONCLUSIONS

We investigated MOR methods to resolve stochastic models consisting of linear dynamical systems with random parameters. The reduction of the larger dynamical system from a stochastic Galerkin method, which was already used in the literature, has been analyzed in more detail. Moreover, we considered MOR of the original dynamical systems followed by the stochastic Galerkin technique as a novel alternative. A respective matrix sampling approach was shown to be feasible in case of moment matching using the Arnoldi algorithm. In addition, we examined parameterized MOR in this context, which enables a further variant. Numerical simulations of test examples demonstrate that all discussed approaches produce reasonable approximations. In particular, the matrix sampling variant offers a high accuracy, whereas the computational effort is relatively low. Parameters that affect the geometry and thus the discretization have not been discussed in this work. We restrict ourselves to refer to [42, 43].

ACKNOWLEDGMENTS

The second author acknowledges the partial financial support from the ENIAC JU Artemos Project /2010/SP2/Wireless communication; Project reference 270683-2, *"Agile Rf Transceivers and front-Ends for future smart Multi-standard cOmmunications applicationS"*, http://www.artemos.eu. Both authors acknowledge the partial financial support from the FP7-ICT-2013-11 Project *"nanoCOPS: Nanoelectronic COupled Problems Solutions"*, under Grant Agreement Number 619166, http://fp7-nanocops.eu/.

The authors thank Dr. Ulrike Baur (MPI, Magdeburg) for helpful discussions on the anemometer example, Dr. Lihong Feng (MPI, Magdeburg) for discussions on pMOR, as well as Prof. Dr. Michael Striebel (HTWG, Konstanz) for the MATLAB code of the RLC circuit example.

REFERENCES

1. Xiu, D. and Karniadakis, G. E., The Wiener-Askey polynomial chaos for stochastic differential equations, *SIAM J. Sci. Comput.*, 24(2):619–644, 2002.
2. Xiu, D. and Hesthaven, J. S., High order collocation methods for differential equations with random inputs, *SIAM J. Sci. Comput.*, 27(3):1118–1139, 2005.
3. Augustin, F., Gilg, A., Paffrath, M., Rentrop, P., and Wever, U., Polynomial chaos for the approximation of uncertainties: Chances and limits, *Eur. J. Appl. Math.*, 19:149–190, 2008.

4. Ghanem, R. G. and Spanos, P., *Stochastic Finite Elements: A Spectral Approach*, Springer, New York, 1991.
5. Xiu, D., *Numerical Methods for Stochastic Computations: A Spectral Method Approach*, Princeton University Press, Princeton, 2010.
6. Pulch, R., Modelling and simulation of autonomous oscillators with random parameters, *Math. Comput. Simulat.*, 81:1128–1143, 2011.
7. Pulch, R., Polynomial chaos for linear differential algebraic equations with random parameters, *Int. J. Uncertainty Quantification*, 1(3):223–240, 2011.
8. Pulch, R., Polynomial chaos for semi-explicit differential algebraic equations of index 1, *Int. J. Uncertainty Quantification*, 3(1):1–23, 2013.
9. Antoulas, A. C., *Approximation of Large-Scale Dynamical Systems*, SIAM, Philadelphia, 2005.
10. Benner, P., Hinze, M., and ter Maten, E. J. W., *Model Reduction for Circuit Simulation*, Lecture Notes in Electrical Engineering, Vol. 74, Springer, Berlin, 2011.
11. Schilders, W. H. A., van der Vorst, M. A., and Rommes, J., *Model Order Reduction: Theory, Research Aspects and Applications*, Math. in Industry Vol. 13, Springer, Berlin, 2008.
12. Baur, U., Beattie, C., Benner, P., and Gugercin, S., Interpolatory projection methods for parameterized model reduction, *SIAM J. Sci. Comput.*, 33:2489–2518, 2011.
13. Benner, P. and Feng, L., A robust algorithm for parametric model order reduction based on implicit moment matching, In *Reduced Order Methods for Modeling and Computational Reduction*, A. Quarteroni and G. Rozza (eds.), Series MS&A (Modeling, Simulation and Applications), Vol. 9, Ch. 6, pp. 159–186, Springer, Berlin, 2014.
14. Bond, B. N. and Daniel, L., A piecewise-linear moment-matching approach to parameterized model-order reduction for highly nonlinear systems, *IEEE Trans. CAD Integr. Circuits Syst*, 26(12):2116–2129, 2007.
15. Villena, J. F. and Silveira, L. M., SPARE—A scalable algorithm for passive, structure preserving, parameter-aware model order reduction, *IEEE Trans. CAD Integr. Circuits Syst*., 29(6):925–938, 2010.
16. Pulch, R., ter Maten, E. J. W., and Augustin, F., Sensitivity analysis and model order reduction for random linear dynamical systems, *Math. Comput. Simulat*., 111:80–95, 2015.
17. Boyaval, S., Bris, C. L., Maday, Y., Nguyen, N. C., and Patera, A. T., A reduced basis approach for variational problems with stochastic parameters: Applications to heat conduction with variable Robin coefficient, *CMAME*, 198(41-44):3187–3206, 2009.
18. Haasdonk, B., Urban, K., and Wieland, B., Reduced basis methods for parameterized partial differential equations with stochastic influences using the Karhunen-Loève expansion, *SIAM/ASA J. Uncertainty Quantification*, 1(1):79–105, 2013.
19. Mi, N., Tan, S. X.-D., Liu, P., Cui, J., Cai, Y., and Hong, X., Stochastic extended Krylov subspace method for variational analysis of on-chip power grid networks, *Proc. IEEE/ACM International Conf. on Computer-Aided Design (ICCAD)*, pp. 48–53, San Jose, CA, Nov. 2007.
20. Zou, Y., Cai, Y., Zhou, Q., Hong, X., Tan, S. X.-D., and Kang, L., Practical implementation of the stochastic parameterized model order reduction via Hermite polynomial chaos, *Proc. ASP-DAC*, pp. 367–372, 2007.
21. Freund, R., Model reduction methods based on Krylov subspaces, *Acta Num.*, 12:267–319, 2003.
22. Ho, C. W., Ruehli, A., and Brennan, P., The modified nodal approach to network analysis, *IEEE Trans. Circuits Syst.*, 22(6):504–509, 1975.
23. Pulch, R. and Xiu, D., Generalised polynomial chaos for a class of linear conservation laws, *J. Sci. Comput.*, 51(2):293–312, 2012.
24. Ernst, O. G., Mugler, A., Starkloff, H. J., and Ullmann, E., On the convergence of generalized polynomial chaos expansions, *ESAIM: Math. Modell. Num. Anal.*, 46:317–339, 2012.
25. Benner, P. and Schneider, J., Uncertainty quantification for Maxwell's equations using stochastic collocation and model order reduction, Report MPIMD/13-19, Max Planck Institut, Magdeburg, Germany, 2013.
26. Eigel, M., Gittelson, C., Schwab, Ch., and Zander, E., Adaptive stochastic Galerkin FEM, *Comput. Methods Appl. Mech. Eng.*, 270:247–269, 2014.
27. Freund, R., Recent advances in structure-preserving model order reduction, In *Simulation and Verification of Electronic and Biological Systems*, P. Li, L. M. Silveira, and P. Feldmann (eds.), Springer, Dordrecht, pp. 43–70, 2011.

28. Gugercin, S., Antoulas, A. C., and Beattie, C., $\mathcal{H}_2$ Model reduction for large-scale linear dynamical systems, *SIAM J. Matrix Anal. Appl.*, 30(2):609–638, 2008.
29. Van Dooren, P., Gramian based model reduction of large-scale dynamical systems, In *Numerical Analysis 1999*, G. A. Watson and D. F. Griffiths (eds.), Series Research Notes in Mathematics, No. 420, Chapman & Hall/CRC, Boca Raton, FL, pp. 231–247, 2000.
30. Haasdonk, B., Convergence rates of the POD-Greedy method, *ESAIM: Math. Modell. Num. Anal.*, 47(3):859–873, 2013.
31. Conrad, P. R. and Marzouk, Y. M., Adaptive Smolyak pseudospectral approximations, *SIAM J. Sci. Comput.*, 35(6):A2643–A2670, 2013.
32. Doostan, A., Owhadi, H., Lashgari, A., and Iaccarino, G., Non-adapted sparse approximation of PDEs with stochastic inputs, *J. Comput. Phys.*, 230(8):3015–3034, 2011.
33. Hairer, E. and Wanner, G., *Solving Ordinary Differential Equations*, Vol. 2: Stiff and Differential-Algebraic Equations, 2nd ed., Springer, Berlin, 1996.
34. Feng, L., Rudnyi, E., and Korvink, J., Preserving the film coefficient as a parameter in the compact thermal model for fast electro-thermal simulation, *IEEE Trans. Comput.-Aided Design Integr. Circuits Syst.*, 24(12):1838–1847, 2005.
35. Li, P., Liu, F., Li, X., Pileggi, L., and Nassif, S., Modeling interconnect variability using efficient parametric model order reduction, In *Proc. of Design Automation and Test In Europe Conference (DATE)*, pp. 958–963, 2005.
36. Voß, T., Verhoeven, A., Bechtold, T., and ter Maten, E. J. W., Model order reduction for nonlinear differential algebraic equations in circuit simulation, In *Progress in Industrial Mathematics at ECMI*, L. L. Bonilla, M. Moscoso, G. Platero, and J. M. Vega (eds.), Mathematics in Industry Vol. 12, Springer, Berlin, pp. 518–523, 2007.
37. http://www.modelreduction.org, Date of retrieval: May 21, 2015.
38. Moosmann, C., Rudnyi, E. B., Greiner, A., and Korvink, J.G., Model order reduction for linear convective thermal flow, In THERMINIC, Sophia Antipolis, France, pp. 317–321, 2004.
39. Saadvandi, M., *Passivity Preserving Model Reduction and Selection of Spectral Zeros*, Master Thesis, KTH, Stockholm, 2008.
40. Günther, M. and Feldmann, U., CAD based electric circuit modeling in industry I: Mathematical structure and index of network equations, *Surv. Math. Ind.*, 8:97–129, 1999.
41. Stroud, A., *Approximate Calculation of Multiple Integrals*, Prentice Hall, Englewood Cliffs, NJ, 1971.
42. Drohmann, M., Haasdonk, B., and Ohlberger, M., Reduced basis method for finite volume approximation of evolution equations on parameterized geometries, *Proc. Algoritmy*, pp. 111–120, 2009.
43. Stavrakakis, K. K., Model order reduction methods for parameterized systems in electromagnetic field simulations, PhD Thesis, TU-Darmstadt, 2012.